Biophys Struct Mech (1982) 8:213–230

Biophysics of Structure and Mechanism

On the Rise Time of the R_1-Component of the "Early Receptor Potential": Evidence for a Fast Light-Induced Charge Separation in Rhodopsin

H.-W. Trissl

Universität Osnabrück, Schwerpunkt Biophysik,
Albrechtstrasse 28, D-4500 Osnabrück, Federal Republic of Germany

Abstract. The rising phase of the R_1-component of the early receptor potential from isolated cattle retinas was measured with high time resolution. When the measuring capacitance was 133 pF, a latency of about 200 ns was observed. A rise time of about 0.8 μs at 0° C and 1.6 μs at 37° C (extrapolated to ideal measuring conditions) was found. The negative temperature dependence indicates that the rise is not directly related to the production and decay of photolysis products of rhodopsin since the latter have positive temperature coefficients. An increase of the external measuring capacitance caused a slower rise time. The analysis of this effect allowed the determination of the source impedance of the R_1-component. The experimental results can be described with a model in which it is assumed that a fast charge separation (ns or ps) takes place in the outer segment of a photoreceptor cell, and spreads passively to the inner segment via the resistance of the interconnecting cilium. The "inner" relaxation could be circumvented by using isolated rod outer segments which lack the passive inner segments, i.e., a rise time of 90 ns could be measured when isolated rod outer segments were attached to Millipore filters. The results suggest that the molecular event leading to the R_1-component is an early charge separation which may be as fast as the cis-trans isomerization of the retinal chromophore.

Key words: Early receptor potential – Fast photovoltage – Rhodopsin – Charge separation

Introduction

Recently a model for the primary events of rhodopsin photolysis was proposed in which light energy is assumed to be stored in the form of a charge separation accompanying the cis-trans isomerization of the retinal chromophore (Honig et al. 1979). The charge separation is thought to be due to the cleavage of a salt

0340-1057/82/0008/0213/$ 03.60

bridge (Honig et al. 1976, 1979; Honig 1978), although a proton translocation is also in discussion (Favrot et al. 1979; Rentzepis 1978; Warshel 1978). An electrical signal as the primary event was suggested by Salem and Bruckmann (1975). Up to now the experimental evidence for this model has been exclusively derived from spectroscopical data. Since a charge separation is equivalent to a change of the molecular dipole moment, one would expect a change of the interfacial potential in membranes containing rhodopsin, provided the dipole is not in plane with the membrane. We know that rhodopsin is asymmetrically embedded in the photoreceptor cell membranes (Clark and Moldau 1979). Therefore, an asymmetrical change of the interfacial dipole potential – which is faster than the discharge time of the membrane – will lead to a change of the transmembrane potential. Such "capacitative" voltage signals have been detected in retinas and photoreceptor cells by flash-illumination. They are known as the "early receptor potential" or ERP (Brown and Murakami 1964; Cone 1964).

The ERP consists of two components, called R_1 and R_2, with opposite polarities and different temperature sensitivities. Whereas the R_2-component is almost entirely suppressed at temperatures below $\sim 10°$ C, the R_1-component is still observable at $-35°$ C (Pak and Ebrey 1965). The rise time of the earlier, corneal-positive R_1-component was found to be ~ 2 µs as measured in the electroretinogram of the isolated rat retina (Cone 1969; Cone and Pak 1971). In view of the above consideration it might be speculated that the molecular origin of R_1 is a primary charge separation taking place in the order of picoseconds. If this were the case, the discrepancy between expected ps and measured µs must be understood. One possible explanation could be the following: in a retina the originally fast signal might be slowed down by electrical relaxation processes within the photoreceptor cell before it can be picked up by external electrodes.

In this communication, evidence for such a fast charge displacement in the rhodopsin-containing photoreceptor cell membranes is reported. However, the signal originating from the outer segment must transverse the retina. In so doing, it is shaped by the connection of the inner segment to the outer segment: the photoelectrically active outer segment membrane charges the passive inner segment membrane via the resistance of the interconnecting cilium. Under ideal measuring conditions this "inner" relaxation time was found to be about 1 µs. This concept predicts that the "inner" relaxation should be bypassed by detachment of the inner segment from the outer segment, as is the case for isolated rod outer segments. When the latter were attached to a Millipore filter separating two aqueous phases (Lindau et al. 1980), a rise time of the photovoltage of 90 ns was found.

Materials and Methods

Cattle eyes were supplied from the local slaughter house and stored for 1–4 h in complete darkness until use. To achieve mechanical stability, isolated retinal slices of 8×12 mm were supported on a filter paper (Schleicher und Schüll, Nr.

604). The retina, together with the filter paper, was clamped between two measuring cells made of black Kel F. Both cells had glass windows for light entrance and light exit and had inner apertures of 0.11 cm^2. In some experiments, a different cuvette was used which had an inner aperture of 0.64 cm^2. The cuvettes were mounted in a thermostatted Faraday-cage.

The photovoltages were measured using light-shielded Ag/AgCl electrodes (electrode resistance < 1 kΩ) with either a 1 MHz electrometer amplifier (input resistance 10^{13} Ω; input capacitance 5.5 pF) or with a 600 kHz low noise voltage amplifier (Ithaco, model 167; input resistance 10^8 Ω; input capacitance 20 pF). Both amplifiers were connected directly to the electrodes without using a cable. Different settings of the external capacitance were achieved by soldering additional capacitors in parallel with the electrodes. The stray capacitance of the cell was 7.5 pF. The numerical values of the external capacitance given in the text include all stray capacitances as well as the preamplifier input capacitance. Most of the photovoltage signals were recorded on a fast storage oscilloscope and then photographed. Alternatively, the photovoltage was stored on a transient recorder (Biomation, model 6500) and averaged on a digital signal analyzer (Tracor Northern, model TN-1500) in order to increase the signal to noise ratio (see Fig. 5).

A laser flash from a frequency doubled Neodym-Yag laser (J K Lasers, system 2000) of 10 ns duration was used for excitation. The flash (wavelength 530 nm) was delivered to the retina by means of a light pipe with random fibers to ensure homogeneous illumination of the retina. The dependence of the amplitude of the R_1-component at 0° C on the relative flash energy is shown in Fig. 2. All other experiments were carried out at relative flash energies between 1.5 and 2.0. This energy range provided a reasonable compromise between a maximal amplitude and a minimal reisomerization of the photolysis products of rhodopsin.

If not mentioned otherwise, the retinas were bathed in an electrolyte solution containing 130 mM NaCl, 10 mM phosphate buffer, pH 7.0. Cattle rod outer segments were prepared according to Schnetkamp et al. (1979). Millipore filters of 0.5 μm pore size were purchased from Satorius.

Results

Original Recordings of the ERP

Usually the corneal-positive R_1-component of the ERP is recorded at low temperatures ($T \approx 0°$ C) where it appears isolated from the R_2-component (Pak and Cone 1964; Pak and Ebrey 1965, 1966; Arden et al. 1968). With increasing temperature, however, R_1 decreases in amplitude and duration, and at 37° C its amplitude is very small or even undetectable (Cone and Pak 1971; Tamai and Holland 1974). Such diminution of the R_1-component with increasing temperature might be ascribed to a poor time resolution of the experiments; i.e., low upper limiting frequencies (10–100 kHz) and flashes of long duration were used.

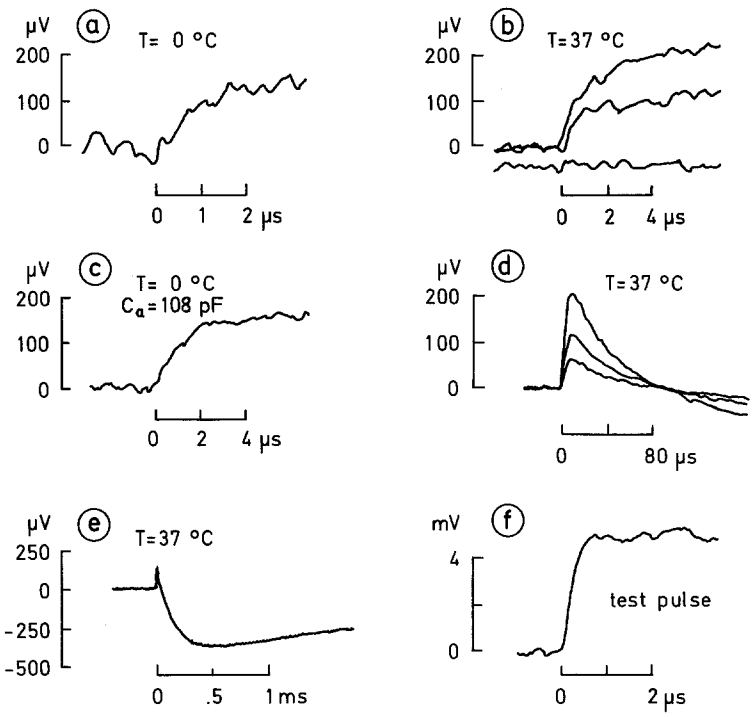

Fig. 1a–f. Original records of the ERP from isolated cattle retinas. The retinas were bathed in 130 mM NaCl, 10 mM phosphate buffer, pH 7.0. A laser flash (λ_{ex} = 530 nm; 10 ns) was applied at $t = 0$. **a** Temperature, $T = 0°$ C; external capacitance, C_a = 13 pF; recording bandwith; 1 MHz. **b** Like **a** but $T = 37°$ C and C_a = 13 pF. The signals of decreasing amplitudes belong to the first, second, and twelfth flash to the same retina. **c** Like **a** but with an external capacitance of C_a = 108 pF. **d** Records of the first, second, and third flash at 37° C in the 100 μs time range. C_a = 28 pF; bandwidth, 100 kHz. **e** ERP at 37° C in the millisecond time range showing the positive R_1-component and the negative R_2-component. **f** Rise time of set-up with a mounted retina and using the 1 MHz electrometer amplifier as tested with a step function (8 ns rise-time) of a pulse generator

When a cattle retina was illuminated by a 10 ns laser flash and the voltage across the retina measured with a recording system of 1 MHz bandwith, the R_1-component could be recorded at 0° C and 37° C with almost equal amplitude as demonstrated in Fig. 1a and b. Since 1 MHz corresponds to a 10%–90% rise time of 350 ns, both signals can be considered as being time resolved with respect to the recording device (see Fig. 1f). Changing the external resistance between 10^6 Ω and 10^{13} Ω influenced neither the shape of the rising phase nor its amplitude (data not shown). In some experiments it was checked that the direction of the light incidence had no influence on the shape or the polarities of the signals.

Repetitive flashes given to the same retina led to decreasing amplitudes. An example is shown in Fig. 1b for the second and 12th flashes. The decrease is also

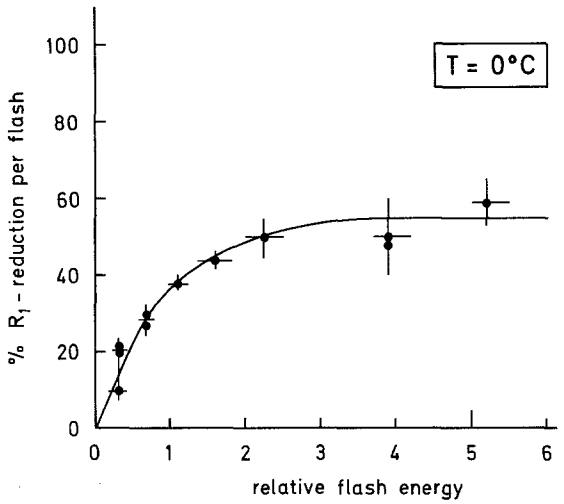

Fig. 2. The decrease of the maximal R_1 amplitude evoked by the first and second flash of single retinas as a function of the flash energy

noticeable in the traces shown in Fig. 1d. The percentage of the diminution between the response of the first and second flash depended on the flash energy as shown in Fig. 2. The saturation at about 50% indicated that, irrespective of the flash energy, no more than one half of the sum of all photovoltage from a retina can be evoked with a single flash. This result is explained by the establishment of a cis-trans isomerization equilibrium of the retinal chromophore during the 10 ns period of excitation (Hagins 1955; Ebrey 1968).

The high time resolution of the experimental set-up used in the present study allowed a proper recording of the time range where the R_1-component passes into the R_2-component at high temperatures. This region is characterized by a change of the sign of the photovoltage. At 37° C, the polarity change occurred at about 80 μs after the flash and did not depend on the number of flashes already delivered to the retina (Fig. 1d). The fully developed R_2-component at 37° C is shown in Fig. 1e on a compressed time scale of milliseconds.

A comparison of Fig. 1a and b reveals that the rise time of R_1 was about twice as long at 37° C than at 0° C. At intermediate temperatures the rise time increased with increasing temperatures (data not shown). An opposite temperature dependence of the rise time would be expected if the time course would be determined by one of the transitions between different photolysis products of rhodopsin, since they all have negative temperature coefficients. This observation raises the possibility that another process governs the rising phase, for instance an electrical relaxation.

This problem was approached by determining the source impedance of R_1 by means of a variation of the external measuring capacitance. It was found that the rise was about twofold slower when the external capacitance was 108 pF instead of 13 pF (compare Fig. 1a and c). In contrast, the amplitude of R_1 was not significantly affected by this change of the measuring condition (see also Fig. 3b).

Dependence of R_1 on the Measuring Capacitance

The slower rise of the R_1-component at the higher measuring capacitance (Fig. 1a and c) can be understood by the assumption that the photovoltage leaves the retina via an "inner" resistance (R_i in Fig. 4) through which the measuring capacitance is charged with the corresponding $R \cdot C$-time constant. If so, it should be possible to determine the source impedance of the component R_1 by systematically varying the measuring capacitance, C_a. In the following, the source impedance is split into a source resistance, R_i, and a source capacitance, C.

In order to quantify the rising phase, we define a rise time, τ_m, as the time at which the signal had developed to $2/e$ of the maximal amplitude (see Fig. 5). In view of the poor signal noise ratio and the rather high variability of different retinas it is not reasonable to correct this rise time for the limiting frequency of the amplifier, for multiexponentials or for a delay time observed at high external capacitances (Fig. 5).

The dependence of the rise time on the external capacitance is shown in Fig. 3a for the temperature $T = 0°$ C (filled circles) and $T = 37°$ C (open circles). The data points in Fig. 3a corresponding to the two temperatures were fitted with linear regression lines. This approximation is discussed below and in the Appendix. The extrapolations to ideal measuring conditions (i.e., $C_a \rightarrow 0$) yield rise times of 0.8 µs at 0° C and 1.6 µs at 37° C. The finite rise times appear to result from a $R \cdot C$ time constant consisting of a source resistance or inner resistance, R_i, through which the external capacitance, C_a, must be charged (Fig. 4). As will be shown in the Appendix, an approximate value for R_i can be calculated from the slope of the regression line in Fig. 3a according to:

$$\Delta\tau = R_i \cdot \Delta C_a \tag{1}$$

Using this equation, a source resistance of $R_i = 10$ kΩ is calculated for the two temperatures. Since the resistance of the retinas and the electrodes were smaller than 1 kΩ in all experiments (measured at 300 kHz), the result infers that the calculated source resistance originates from within the retina. One should bear in mind that this resistance belongs specifically to the R_1 generating process.

To explain Fig. 3a, the photovoltage was assumed to leave the retina via an inner source resistance and, since it is generated in or at membranes, it is reasonable to assume also a source capacitance, C. The magnitude of such a capacitance can be estimated from the peak amplitudes of the R_1-component at different values of the external capacitance, C_a. This was achieved by assuming a simple equivalent circuit composed of two capacitors connected in parallel. At zero time one capacitor, C, is charged with a given charge yielding the voltage V_0 which subsequently equilibrates with the other capacitor, C_a. After the system has relaxed, the steady state voltage, V, can be calculated according to a capacitative voltage divider:

$$\frac{1}{V} = \frac{1}{V_0} + \frac{1}{V_0 \cdot C} C_a \,. \tag{2}$$

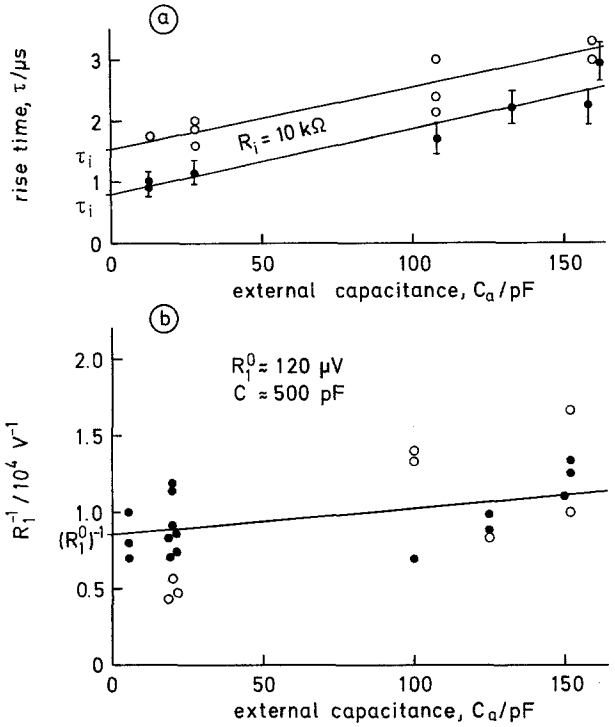

Fig. 3. Dependence of the rise time of the R_1-component on the external capacitance, C_a, at $T = 0°$ C (filled circles) and $T = 37°$ C (open circles). The rise time is defined in the text and in Fig. 5. Extrapolation to ideal measuring conditions ($C_a \to 0$) yields the "inner" relaxation time constant, τ_i. Data fitted by linear regression. Correlation coefficient $r = 0.90$ (37° C) and $r = 0.96$ (0° C). **b** Dependence of the reciprocal maximal amplitude of R_1 on the external capacitance C_a at $T = 0°$ C (filled circles) and $T = 37°$ C (open circles). The parameters in the inset represent the mean value of the maximal R_1 amplitude under ideal measuring conditions and the mean value of the corresponding source capacitance as calculated by a linear regression of the data at $T = 0°$ C and using (3). Correlation coefficient $r = 0.51$. At a confidential level of 80% the deviations from the mean values are $R_1^0 = 119^{+14}_{-13}$ μV and $C = 496^{+704}_{-185}$ pF

The equation can be applied when resistors parallel to the capacitors are sufficiently large so that a steady state value of the voltage can develop before a $R \cdot C$ decay process starts. This condition is satisfied for the experiments at $T = 0°$ C, though not as well at $T = 37°$ C (Fig. 1d).

According to (2), the reciprocal amplitudes of R_1 in 16 experiments at 0° C and seven experiments at 37° C are plotted in Fig. 3b versus C_a. For the reasons mentioned above, only the data points corresponding to 0° C were analyzed. The linear regression yields values of $V_0 = 119^{+9}_{-7}$ μV and $C = 496^{+342}_{-148}$ pF at a confidence level of 60%. The large error of the source capacitance is due to variations of the photovoltage with different retinas; such a plot cannot be made with one retina. Nevertheless, it can be stated that the R_1 amplitude is almost independent of the external capacitance within the tested range of C_a, i.e., $C \gg C_a$. In a first approximation, therefore, R_1 can be considered to originate

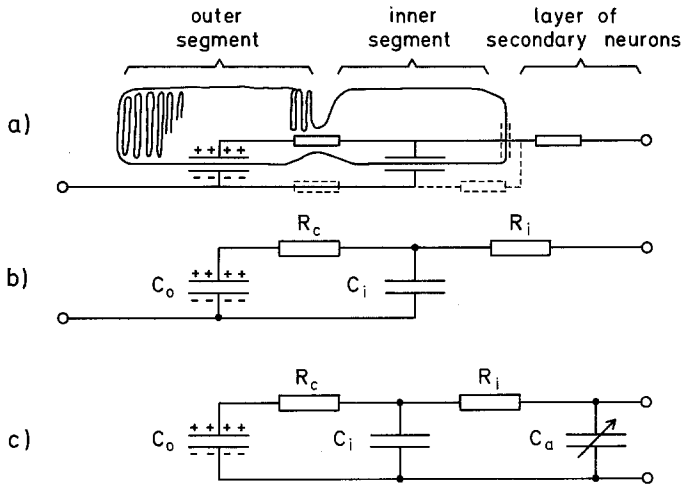

Fig. 4a–c. Derivation of an equivalent electrical circuit form a rod type photoreceptor cell. C_0 = capacitance of the plasma membrane of the outer segment; C_i = capacitance of the inner segment; R_c = resistance of the cilium; R_i = resistance of the layer of secondary neurons. **a** Schematic representation of a rod showing the positions of the equivalent capacitors and resistors. The elements drawn with dashed lines are neglected as explained in the text. **b** The separate equivalent circuit. **c** The same equivalent circuit but rearranged and extended by the external capacitance, C_a

from a constant voltage source (battery). Another result contained in Fig. 3b may be noted, namely that the amplitude of R_1 is rather independent of temperature (compare open circles with filled circles).

An Equivalent Circuit

In order to allow an analysis of the basic experimental findings, an equivalent circuit was derived in accordance with the following aspects: (i) it should be composed of as few components (capacitors and resistors) as possible, (ii) it should not be in conflict with the structure of a photoreceptor cell, (iii) it should account for both the finite rise time measured under the assumption of a step function as the generating process and the dependence of the rise time on the external capacitance. Figure 4a illustrates how such a circuit can be derived from a rod type photoreceptor cell. Here, the positions of the equivalent components are shown with respect to the cell structure. The resistor near the cilium, drawn with dashed lines, is assumed to be small and is therefore neglected. The resistor connecting the synaptic body with the region of the cilium (dashed lines) must be high since no discharge occurs within 10 μs and accordingly is also neglected. The ac-resistance (at frequencies $\gtrsim$ 100 kHz) of the series capacitor at the synaptic body is assumed to be smaller than the ohmic resistance, R_i. The latter represents the exit resistance of the fast photovoltage through the layer of secondary neurons.

The connection of the remaining components, i.e., the resistance of the cilium, R_c, the capacitance of the plasma membrane of the outer segment, C_0, and the capacitance of the membrane of the inner segment, C_i, is shown in Fig. 4b. The outer segment plasma membrane is assumed to contain rhodopsin and to be photoelectrically active (as indicated by the charge on C_0), whereas the inner segment membrane is assumed to contain no rhodopsin and to be electrically passive (Hagins and Rüppel 1971; Rüppel and Hagins 1973; Govardovskii 1975).

In Fig. 4c the components of the equivalent circuit are rearranged and the external capacitance, C_a, is included. The equivalent circuit is not intended to describe the exact time course of the R_1-component, nor to represent an electrophysiological relevant receptor model. Its utility lies rather in its ability to mimick systems in which a fast charge separation leads to a slower voltage rise. In the following, this circuit will be considered as an integral over all photoreceptors (rods and cones) of the experimental area. If not otherwise specified, all numerical values of the circuit components given in the text refer to this area (0.11 cm^2). Equivalent circuits basically similar to those in Fig. 4 have been described previously (Arden et al. 1968; Cone 1969; Govardovskii 1978).

A Latency of the Rising Phase

Assuming that the charge displacement at C_0 can be approximated by a step function, the equivalent circuit in Fig. 4c can now be used to calculate the time course of the photovoltage as well as its dependence on the external capacitance. Since the source capacitance of the photovoltage was found to be much larger than the external capacitances used (see Fig. 3b), the step function of the charge separation can be approximated by a step function of voltage. In this case the equivalent circuit (Fig. 4c) reduces to two identical *RC*-four poles (Fig. 7), and thus can be treated with the theory of four-terminal network. The analytical solution for the voltage $V(t)$, is given by (18) in the Appendix. As shown there, this equation allows the derivation of (1) and predicts a latency of the photovoltage for finite values of the external capacitance.

Using (18), the time course of the rising phase can be calculated and compared with that measured. This is shown in Fig. 5 where 12 "first flash" signals at 0° C were averaged to increase the signal to noise ratio (curve 1). The photovoltage was recorded with an external capacitance of 133 pF. Under this condition, a latency of about 200 ns was found. The theoretical curve (curve 2) also shows a latency of the same order. This curve was calculated using the parameters found experimentally: $C_i = 500$ pF, $R_i = 10$ kΩ, and $\tau_i = 0.8$ μs ($= \tau_1$ in the nomenclature of the Appendix). Unfortunately, the data in Fig. 3b do not allow an accurate determination of C_i so that its value might be considerably higher. However, at equal τ_i this would neither influence the shape of the signal nor its dependence on the external capacitance within the experimental accuracy (see also discussion in Appendix). In accordance with the experiments (Fig. 3a) the calculated rise time increases with increasing external capacitances as shown in Fig. 8.

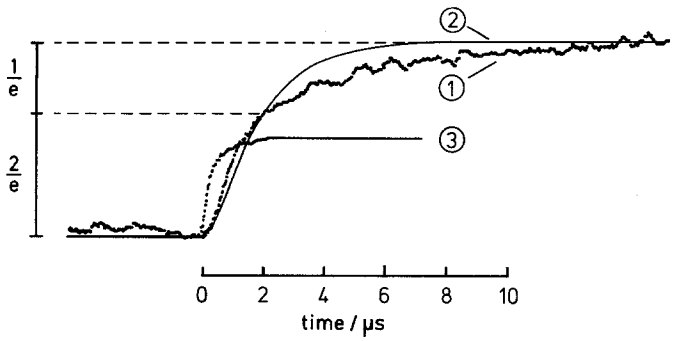

Fig. 5. The rising phase of the R_1-component from cattle retinas at 0° C. Curve (1) represents the average of 12 signals from 12 different retinas measured at an external capacitance of 133 pF and a recording bandwidth of 1 MHz. Only the first flash to a retina was used. Curve (2) was calculated according to (18) using the parameters: $C_i = 500$ pF, $R_i = 13$ kΩ, $\tau_i = 0.8$ µs and $C_a = 133$ pF. Curve (3) is the integrated time course of the laser flash as measured with a fast photodiode (step function). The signal of the photodiode was amplified and displayed with the identical amplifier and recording system as used for curve (1)

C_i, R_i, and τ_i completely determine the theoretical curve in Fig. 5. Evidently, the measured and calculated time courses differ somewhat. The differences, however, may not be surprising in view of the simplifications made for the equivalent circuit. For instance, the possible contribution of different photoreceptor cells, cones and rods, are neglected. On the other hand, the theoretical treatment reproduces the main features of the experimental findings, i.e., the latency of the photovoltage and the dependence of the rise time on the external capacitance.

Experiments with Isolated Rod Outer Segments

In the foregoing, the photovoltages obtained from retinas were mimicked theoretically by an initial voltage step and a subsequent relaxation within a photoreceptor cell. The relaxation was assumed to occur by the interaction between the active outer segment and the passive inner segment. This hypothesis predicts that a faster rise time with no latency period would be measured when the inner segment is removed from the outer segment, as is the case for isolated rod outer segments (ROS). Recently, an experimental system was described which makes such a measurement possible: isolated ROS's can be attached to one side of a cellulose nitrate filter yielding partially oriented membrane fragments (Lindau et al. 1980). The photovoltage responses from this system closely resemble the ERP from retinas.

To test the above prediction, filters impregnated with isolated ROS were placed in the same measuring cuvette as used for the retinas. The photovoltage was measured with a 10 MHz preamplifier (total stray capacitance 13 pF) and is shown in Fig. 6. To increase the signal to noise ratio, four signals were averaged.

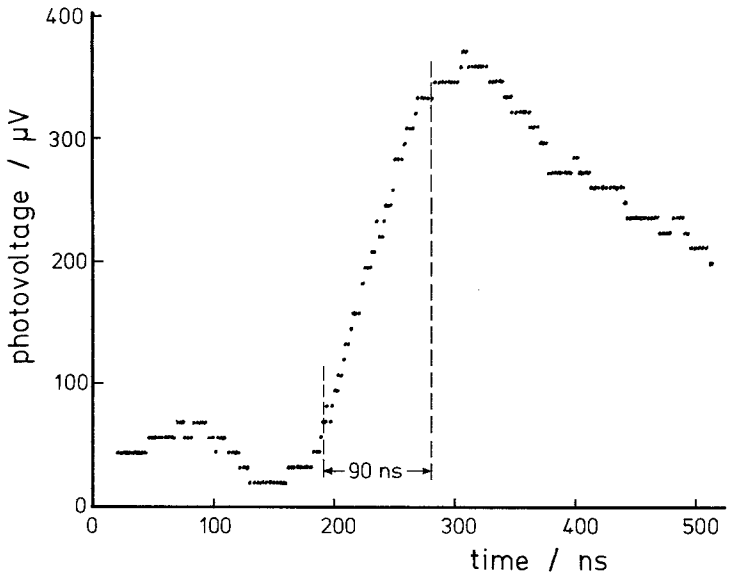

Fig. 6. Photovoltage from isolated rod outer segments attached to Millipore filters. To achieve a high conductance the electrolyte was 1 M NaCl, 10 mM phosphate buffer, pH 7.0. Four signals were averaged resulting from the first laser flashes to four freshly impregnated filters. The signals were preamplified with a 10 MHz electrometer amplifier, then with a 5 MHz amplifier and recorded with a transient recorder (2 ns/point). Recording bandwidth: 5 MHz; external capacitance, C_a = 13 pF

In this particular experiment a 10%−90% rise time of 90 ns was measured with no significant latency. As was observed with retinas the first flash evoked a photopotential in the order of 100 μV and subsequent flashes evoked signals of decreasing amplitudes. Different impregnated filters displayed variations of the rise time on the order of 50%. In these experiments it was noticed that the rise time decreased with increasing amounts of ROS attached to the filter, indicating that the measured rise time is electrically limited by the system. Nevertheless, this experiment, which demonstrates a 10 times faster rise time of ROS as compared with retinas, justifies the above assumption that a fast charge separation (step function) is the generating process of the R_1-component in retinas.

The experiment does not exclude the possibility, that the 90 ns rise time is related to the bathorhodopsin-lumirhodopsin transition. At room temperature this transition was reported to occur within 30−170 ns, depending on the reference (Bensasson et al. 1975, 1977; Busch et al. 1972; Cone 1972; Goldschmidt et al. 1976; Rosenfeld et al. 1972). Given these discrepancies in the reported time range of the batho-lumirhodopsin transition, and the fact that the measured rise time of 90 ns is not time resolved, it is not possible at present to decide whether the fast charge separation dealt with in this communication is an early ps event or is related to the decay of the first stable photolysis product bathorhodopsin.

Discussion

This paper reports the first observation of a latency of the R_1-component of the ERP from retinas. Such an observation was made possible by the very fast resolution time of the recording electronics. It was found that the latency and the rise time depended on the external measuring capacitance, both decreasing as the capacitance was lowered. This result indicates that these quantities are governed by electrical interaction of the photoreceptor cells with the measuring amplifier rather than by rate constants of a conformational transition in the photolysis of rhodopsin.

It has been argued that an early charge separation in rhodopsin most likely occurs as one of the primary events (Salem and Bruckmann 1975; Honig et al. 1979). Since rhodopsin is asymmetrically embedded in the membranes of photoreceptors (Röhlich 1976; Clark and Moldau 1979), such charge separation can be expected to produce a measurable photovoltage. Furthermore, the charge separation probably occurs within ps and, accordingly, the true time course of the photovoltage will be as fast. However, the rise time measured in this study was only 0.8 μs, and a latency was shown to exist under real measuring conditions. These data were explained by the following assumptions of electrical properties of photoreceptor cells in a retina: (i) charge has to equilibrate between the membranes of the photoelectrically excited outer segment and the passive inner segment through the resistance of the cilium. This causes the finite rise time at $C_a = 0$! (ii) The signal thus relaxed leaves the retina via another resistance, R_i, which represents an ohmic resistance for the R_1-component through the layer of secondary neurons. This resistance together with the external capacitance causes the latency! It should be stressed that the R_1-shaping cannot be ascribed to the impedance of the whole retina (Fig. 1f) but is specifically due to the R_1-signal of photoreceptor cells.

From these considerations it can be deduced that the underlying molecular process must be much faster than these relaxation times. This concept is strongly supported by the experiments with isolated rod outer segments (lacking the passive inner segment) in which a rise time of 90 ns was measured. It is conceivable that an even higher time resolution may be achieved by other methods, for instance the monolayer technique developed by the author (Trissl 1980). Up to now the latter method yielded only very small R_1-like photovoltages which could not be subjected to a rise time analysis.

Further support for the suggestion that the finite rise time represents an electrical relaxation comes from the negative temperature dependence observed for the rising phase of R_1. A negative temperature dependence implies that the rising phase cannot be identified with one of the different transitions in the photolysis of rhodopsin, as the latter all have positive temperature coefficients (Ostroy 1977). One possible explanation of the negative temperature dependence would be that the resistance of the cilium determines the finite rise time. This resistance could be largely determined by the cell geometry. Thus, it might be conceivable that the sectional area of the cilium decreases with increasing temperature, resulting in a larger R_c (see Fig. 4) and therefore a larger time constant. If such shrinkage of the diameter of the cilium at higher temperatures

is indeed responsible for the negative temperature dependence, an Arrhenius plot of the time constant of the rising phase would be meaningless.

When the rising phase is assumed to reflect an electrical relaxation within each photoreceptor cell, one expects the rise time to be independent of the number of cells in parallel, i.e., of the absolute area of the retinal slice (in the limit of $C_a \rightarrow 0$). Corresponding control experiments in which the area of the retina was chosen to be 6-fold larger than usual (0.64 cm^2 instead of 0.11 cm^2) showed that the maximal amplitude of R_1, as well as the rise time, were the same within the experimental accuracy (measuring conditions: $T = 0°$ C; $C_a = 13$ pF; data not shown).

Another argument in favour of the outlined concept is the experimental observation that the rise time was independent of the conductance of the bathing medium (examined range: 60–240 mM NaCl; data not shown).

It is of interest at this point to notice that the above interpretation implies that the outer segment and the inner segment are equipotential within some microseconds. Compared with the experiments of Bader et al. (1979) on isolated tiger salamander rod cells, this value represents an increase of time resolution of almost three orders of magnitude.

From the measured value of $R_i \approx 10^4\ \Omega$ it is possible to estimate the source resistance for the R_1-component of one "mean photoreceptor cell". The number of photoreceptors in a typical slice of retina was determined using a phase contrast microscope to be about $10^7\ cm^{-2}$. Since R_i does not represent the resistance of the retina (approximately 100–200 Ω for the area used in the experiments), the effective R_1-source resistance of a single photoreceptor cell in a cattle retina is therefore in the order of 10 GΩ. It should be mentioned that a corresponding normalization for the resistance of the cilium, R_c, and for the membrane capacitance of the inner segment, C_i, is not feasible since both quantities enter into the analysis as a product [$\tau_i = R_c \cdot C_i$; see also (15)]. The present data do not allow the determination of R_c and C_i separately.

The above estimation of R_i suffers from the poorly defined term "mean photoreceptor", since the cattle retina is composed of rods and cones. The extent to which both cell types contribute to the fast rise is unknown. In rod- or cone-dominated eyes, the ERP appears very similar (Pak and Ebrey 1966). Although the cones in mixed retinas are much less abundant than rods, they usually contribute more than 50% to the ERP. According to an investigation on the rod and cone contribution in human eyes by Zanen and Debecker (1975), the R_1-component is predominantly produced by cones. If it is assumed that both cell types in cattle retinas are similarly effective in producing R_1, but have different time constants, one would expect a multi-phasic rise. This might explain the difference between the calculated and measured rising phase seen in Fig. 5.

In summary, the experimental data and their analysis indicate a fast charge separation (≤ 90 ns) occurring in the dielectric of the rhodopsin-containing photoreceptor membranes. The simple equivalent circuit used for the analysis satisfactorily accounts for the observed latency of the R_1-component from retinas, the dependence of the rise time on the measuring capacitance, and the faster rise time in isolated rod outer segments. Because of the negative

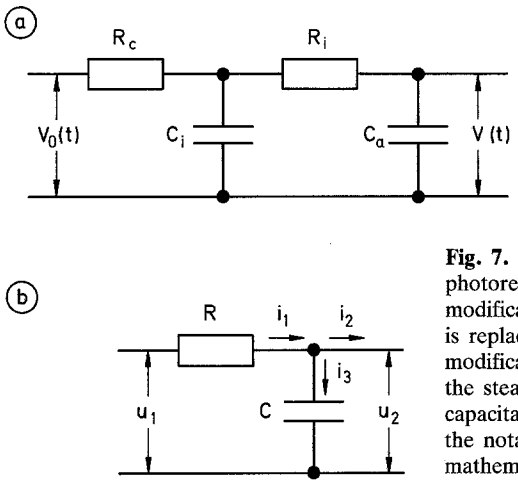

Fig. 7. a Reduced equivalent circuit for a photoreceptor cell as derived from Fig. 4. The modification consists in the omission of C_0 which is replaced by a voltage source, $V_0(t)$. This modification accounts for the independence of the steady state photovoltage on the external capacitance (Fig. 3b). **b** One quadripole showing the notations and definitions used for the mathematical treatment

temperature dependence, the rising phase of R_1 from retinas cannot be correlated to a transition between photolysis products of rhodopsin. However a correlation between the faster 90 ns rising phase in the case of isolated ROS and the decay of bathorhodopsin might be possible.

Appendix

Mathematical Treatment of the Equivalent Circuit

The most appropriate way of mathematically analyzing the equivalent circuit shown in Fig. 4c is to apply the theory of four-terminal network. For this purpose the circuit is modified by substituting the source of the photovoltage at C_0 by a voltage generator of low impedance (not shown) which delivers a step pulse at zero time (Fig. 7a). This yields a series combination of two identical $R \cdot C$ quadripoles. In order to meet the usual nomenclature of four-terminal network, a single quadripole is designed and labeled as shown in Fig. 7b. We now ask for the time course of the output voltage $V(t)$ when the input voltage $V_0(t)$ is a step function at $t = 0$.

A single quadripole (Fig. 7b) is composed of one resistor and one capacitor. The current in each loop obeys the relation

$$i_3 = i_1 - i_2 \,. \tag{3}$$

The impedances of the two elements are

$$z_1 = R \,, \tag{4}$$

$$z_2 = 1/i\omega C = 1/p \cdot C \,, \tag{5}$$

where i is the imaginary unit.

The four-pole equations then read

$$u_1 = i_1 \cdot z_1 + (i_1 - i_2) \cdot z_2 = i_1 \cdot (z_1 + z_2) - i_2 \cdot z_2 \,, \tag{6}$$

$$u_2 = (i_1 - i_2) \cdot z_2 \qquad = i_1 \cdot z_2 \qquad - i_2 \cdot z_2 \,, \tag{7}$$

and in matrix notation:

$$\begin{pmatrix} u_1 \\ u_2 \end{pmatrix} = \begin{pmatrix} z_1 + z_2 & -z_2 \\ z_2 & -z_2 \end{pmatrix} \begin{pmatrix} i_1 \\ i_2 \end{pmatrix} . \tag{8}$$

The quadripole equations are now transformed into a matrix of ladder network in cascade:

$$\begin{pmatrix} u_1 \\ i_1 \end{pmatrix} = \begin{pmatrix} \dfrac{z_1 + z_2}{z_2} z_1 \\ 1/z_2 \quad 1 \end{pmatrix} \begin{pmatrix} u_2 \\ i_2 \end{pmatrix} . \tag{9}$$

Now we connect two quadripoles in series by multiplying the characteristic matrices and labeling the left one with $'$ and the right one with $''$:

$$\begin{pmatrix} u_1' \\ i_1' \end{pmatrix} = \begin{pmatrix} \dfrac{(z_1' + z_2') \cdot (z_1'' + z_2'')}{z_2' \cdot z_2''} + \dfrac{z_1'}{z_2''} & \dfrac{(z_1' + z_2') \cdot z_1''}{z_2} + z_1' \\ \dfrac{1}{z_2'} \dfrac{(z_1'' + z_2'')}{z_2''} + \dfrac{1}{z_2''} & \dfrac{z_1''}{z_2'} + 1 \end{pmatrix} \begin{pmatrix} u_2'' \\ i_2'' \end{pmatrix} . \tag{10}$$

Since the voltmeter used in the experiments is high-ohmic i_2'' can be set to zero. The transfer function for the voltage then reads

$$u_1' = \left(\frac{z_1' + z_2'}{z_2'} \cdot \frac{z_1'' + z_2''}{z_2''} + \frac{z_1'}{z_2''} \right) \cdot u_2'' \tag{11}$$

or in terms of the original notation of the impedances:

$$u_1' = \left(\frac{R_c + 1/p \cdot C_i}{1/p \cdot C_i} \frac{R_i + 1/p \cdot C_a}{1/p \cdot C_a} + \frac{R_c}{1/p \cdot C_a} \right) \cdot u_2'' \,. \tag{12}$$

This equation reduces to the transfer function $u_2''(p)$:

$$u_2''(p) = \frac{1}{p^2 \cdot a + p \cdot b + 1} \cdot u_1' \tag{13}$$

with

$$a = R_c C_i \cdot R_i C_a = \tau_1 \cdot \tau_2 \,, \tag{14}$$

$$b = R_c C_i + R_i C_a + R_c C_a = \tau_1 + \tau_2 + \tau_3 \,. \tag{15}$$

Equations 14 and 15 define the time constants τ_1, τ_2, and τ_3. The Laplace transformation of a step function (Greuel 1972) is

$$u_1'(p) = \frac{V_0}{p}. \tag{16}$$

Therefore

$$u_2''(p) = \frac{V_0}{(p^2 \cdot a + p \cdot b + 1) \cdot p}. \tag{17}$$

The inverse transformation into the original space (time) can be found in text books of Laplace transformations. The normalized output voltage in the notation of time constants (16) and (17) reads

$$\frac{V(t)}{V_0} = 1 - \exp - \left(\frac{\tau_1 + \tau_2 + \tau_3}{2\tau_1\tau_2} \cdot t\right) \cdot \left[\frac{\tau_1 + \tau_2 + \tau_3}{\sqrt{(\tau_1 + \tau_2 + \tau_3)^2 - 4\tau_1\tau_2}} \cdot \right. \tag{18}$$

$$\left. \cdot \sinh \frac{\sqrt{(\tau_1 + \tau_2 + \tau_3)^2 - 4\tau_1\tau_2}}{2\tau_1\tau_2} \cdot t + \cosh \frac{\sqrt{(\tau_1 + \tau_2 + \tau_3)^2 - 4\tau_1\tau_2}}{2\tau_1\tau_2} \cdot t \right].$$

This exact solution contains three time constants, whereas the experimental data were analyzed for only one time constant (see Fig. 5). In order to allow for a comparison, the same procedure was applied to the above equation: for a given set of parameters (R_c, R_i, C_i), the time at which $V(t)$ has reached $1/e$ of its final value was calculated numerically. The dependence of the such defined rise time on the external capacitance is plotted in Fig. 8 for three different values of R_i (10, 13, and 16 kΩ) assuming the parameters $R_c = 1.6$ kΩ and $C_i = 500$ pF. This set of parameters is chosen to meet the experimental data: $C_i \gg C_a$ (Fig. 3b) and $\tau_i = 0.8$ µs [see Fig. 3a and (16)]. The dashed lines in Fig. 8 were drawn according to the approximation

$$\Delta\tau = R_i \cdot \Delta C_a, \tag{1}$$

for $C_a \rightarrow 0$, whereas the smooth lines indicate the exact treatment according to the above definition of the rise time. One can see that the deviation between both treatments is in the order of the experimental deviations, and therefore it is reasonable to apply the approximation of (1).

Note that the numerical values of R_c and C_i refer to the sum of all photoreceptor cells of the experimental area (0.11 cm^2). Consider also that the numerical values of this parameter couple can only be arbitrarily assumed due to the criteria $C_i \gg C_a$ and $R_c \cdot C_i = \tau_i$. Unfortunately, the parameters cannot be determined separately since (18) is sensitive only to τ_1 (= product of R_c and C_i) and τ_2, but not to τ_3, as can be seen from (15): $\tau_3 < \tau_2$! The choice of larger values for C_i and smaller values for R_c so that the product remains 0.8 µs is as good and will yield indistinguishable results.

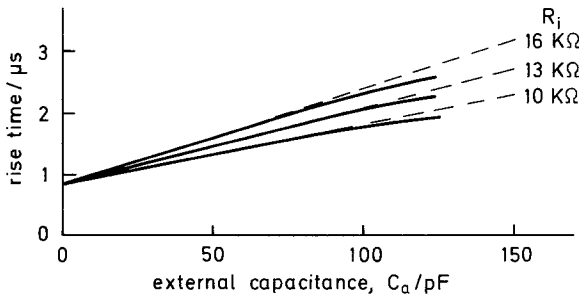

Fig. 8. Dependence of the calculated rise time on the external capacitance for three different values or R_i. The solid curves were calculated with (18) choosing the parameter $\tau_i = 0.8$ µs

A computed time course of the output voltage resulting when the input voltage is a step function is shown in Fig. 5. The curve has an induction phase (latency) which amounts to about 200 ns at $C_a = 133$ pF.

Acknowledgements. I am particularly grateful to Ing. U. Klose for help with the mathematical analysis. I also thank Prof. W. Junge, Dr. B. Kaupp, Prof. L. H. Pinto, Dr. P. P. M. Schnetkamp, and Dr. S. M. Theg for critical discussions and help with the manuscript. The work was financially supported by the Deutsche Forschungsgemeinschaft.

References

Arden GB, Bridges CDB, Ikeda H, Siegel IM (1968) Mode of generation of the early receptor potential. Vision Res 8:3–24

Bader CR, MacLeish PR, Schwartz EA (1979) A voltage-clamp study of the light response in solitary rods of the tiger salamander. J Physiol (Lond) 296:1–26

Bensasson R, Land EJ, Truscott TG (1975) Nanosecond flash photolysis of rhodopsin. Nature 258:768–770

Bensasson R, Land EJ, Truscott TG (1977) Laser flash photolysis of rhodopsin at room temperature. Photochem Photobiol 26:601–605

Brown KT, Murakami M (1964) A new receptor potential of the monkey retina with no detectable latency. Nature 201:626–628

Busch GE, Applebury ML, Lamola AA, Rentzepis PM (1972) Formation and decay of prelumirhodopsin at room temperatures. Proc Natl Acad Sci USA 69:2802–2806

Clark SP, Moldau RS (1979) Orientation of membrane glycoproteins in sealed rod outer segment disks. Biochemistry 18:5868–5873

Cone RA (1964) Early receptor potential of the vertebrate retina. Nature 204:736–739

Cone RA (1969) The early receptor potential. In: Reichardt W (ed) Proc. Int. School of Physics, "Enrico Fermi", Course 43. Academic Press, New York, pp 187–200

Cone RA (1972) Rotational diffusion of rhodopsin in the visual receptor membrane. Nature (New Biol) 236:39–43

Cone RA, Pak WL (1971) The early receptor potential. In: Loewenstein WR (ed) Handbook of sensory physiology, vol 1. Springer, Berlin Heidelberg New York, pp 345–365

Ebrey TG (1968) The thermal decay of the intermediates of rhodopsin in situ. Vision Res 8:965–982

Favrot J, Leclerc JM, Roberge R, Sandorfy C, Vocelle D (1979) Intermolecular interactions in visual pigments. The hydrogen bond in vision. Photochem Photobiol 29:99–108

Goldschmidt CR, Ottolenghi M, Rosenfeld T (1976) Primary processes in photochemistry of rhodopsin at room temperature. Nature 263:169–170

Govardovskii VI (1975) The sites of generation of the early and late receptor potential in rods. Vision Res 15: 973–980
Govardovskii VI (1978) Mechanism of the generation of the early receptor potential and an electrical model of the rod of the rat retina. Biofizika 23: 514–519
Greuel O (1972) Das Fachwissen des Ingenieurs. Mathematische Ergänzungen und Aufgaben für Elektrotechniker. Carl Hanser, München
Hagins WA (1955) The quantum efficiency of bleaching in situ. J Physiol (Lond) 129: 23P
Hagins WA, Rüppel H (1971) Fast photoelectric effects and the properties of vertebrate photoreceptors as electric cables. Fed Proc 30: 64–68
Honig B (1978) Light energy transduction in visual pigments and bacteriorhodopsin. Annu Rev Phys Chem 29: 31–57
Honig B, Greenberg AD, Dinur U, Ebrey TG (1976) Visual pigment spectra: Implications of the protonation of the retinal Schiff base. Biochemistry 15: 4593–4599
Honig B, Ebrey T, Callender RH, Dinur U, Ottolenghi M (1979) Photoisomerization, energy storage, and charge separation: A model for light energy transduction in visual pigments and bacteriorhodopsin. Proc Natl Acad Sci USA 76: 2503–2507
Lindau M, Hochstrate P, Rüppel H (1980) Two component fast photosignals derived from rod outer segment membranes attached to porous cellulose filters. FEBS Lett 112: 17–20
Ostroy SE (1977) Rhodopsin and the visual process. Biochim Biophys Acta 563: 91–125
Pak WL, Cone RA (1964) Isolation and identification of the initial peak of the early receptor potential. Nature 204: 836–838
Pak WL, Ebrey TG (1965) Visual receptor potential observed at sub-zero temperatures. Nature 205: 484–486
Pak WL, Ebrey TG (1966) Early receptor potentials of rod and cones in rodents. J Gen Physiol 49: 1199–1208
Rentzepis PM (1978) Picosecond chemical and biological events. Science 202: 174–184
Röhlich P (1976) Photoreceptor membrane carbohydrate on the intradiscal surface of retinal rod discs. Nature 263: 789–791
Rosenfeld T, Alchalal A, Ottolenghi M (1972) Nanosecond laser photolysis of rhodopsin in solution. Nature 240: 482–483
Rüppel H, Hagins WA (1973) Spatial origin of the fast photovoltage in retinal rods. In: Langer H (ed) Biochemistry and physiology of visual pigments. Springer, Berlin Heidelberg New York, pp 257–261
Salem L, Bruckman P (1975) Conversion of a photon to an electrical signal by sudden polarisation in the N-retinylidene visual chromophore. Nature 258: 526–528
Schnetkamp PPM, Klompmaker AA, Daemen FJM (1979) The isolation of stable cattle rod outer segments with an intact plasma membrane. Biochim Biophys Acta 552: 379–389
Tamai A, Holland MG (1974) Early receptor potential of a typical rod monochromat. Yonago Acta Med 18: 181–190
Trissl H-W (1980) A novel capacitative electrode with a wide frequency range for measurements of flash-induced changes of interface potential at the oil-water interface. Mechanical construction and electrical characteristics of the electrode. Biochim Biophys Acta 595: 82–95
Warshel A (1978) Charge stabilization mechanism in the visual and purple membrane pigments. Proc Natl Acad Sci USA 75: 2558–2562
Zanen A, Debecker J (1975) Wavelength sensitivity of the two components of the early receptor potential (ERP) of the human eye. Vision Res 15: 107–112

Received November 24, 1981/Accepted January 8, 1982